Evidence for 13-carbon enrichment in oxalic acid via iron catalyzed photolysis in aqueous phase

Chandra Mouli Pavuluri[1] and Kimitaka Kawamura[1]

Received 17 November 2011; revised 30 December 2011; accepted 7 January 2012; published 9 February 2012.

[1] To investigate the effect of photochemical aging on the stable carbon isotopic ratio ($\delta^{13}C$) of oxalic acid (OxA), a dominant organic species in atmospheric aerosols, we conducted a laboratory photolysis of OxA under H_2O_2-Fe^{3+}(Fe^{2+})-UV system in aqueous phase and measured $\delta^{13}C$ of remaining OxA. Our results showed that a significant photolysis of OxA occurred with OH radical but the isotopic fractionation of OxA was insignificant. In contrast, in the presence of Fe^{3+} (Fe^{2+}), we found a significant enrichment of ^{13}C in remaining OxA. We also found that kinetic isotope effect (KIE) of OxA largely depends on photochemical age (irradiation time) and concentration ratios of OxA to iron; 3.20 ± 0.49‰ (2.18 ± 1.18‰) and 21.62 ± 5.41‰ in 90 min and 180 min irradiation, in which OxA and Fe^{3+} (Fe^{2+}) ratios were 50:1 and 200:1, respectively. The enrichment of ^{13}C in remaining OxA was more significant during the photolysis catalyzed by Fe^{3+} (7‰) than by Fe^{2+} (3‰) in 90 min irradiation when OxA and iron ratios are the same (50:1). This study provides a laboratory evidence for the isotopic enrichment of ^{13}C in OxA with photochemical aging. This approach is useful for better interpretation of atmospheric isotopic measurements in terms of the extent of atmospheric processing of aerosols. **Citation:** Pavuluri, C. M., and K. Kawamura (2012), Evidence for 13-carbon enrichment in oxalic acid via iron catalyzed photolysis in aqueous phase, *Geophys. Res. Lett.*, *39*, L03802, doi:10.1029/2011GL050398.

1. Introduction

[2] Oxalic acid (OxA) is the most abundant species among a series of dicarboxylic acids in atmospheric particles. Its concentrations range from 10 ng m^{-3} to 70 ng m^{-3} in remote regions [*Kawamura et al.*, 1996a, 1996b], and up to 1300 ng m^{-3} in urban air [*Ho et al.*, 2007] and 2000 ng m^{-3} in biomass burning impacted aerosols [*Kundu et al.*, 2010]. Due to very water-soluble and hygroscopic properties of OxA [*Peng et al.*, 2001], its existence on the aerosol surface alters the chemical and physical properties of the atmospheric aerosols and enhances the capability of aerosols to act as cloud condensation nuclei [*Kawamura and Usukura*, 1993; *Saxena et al.*, 1995] and thus affect the climate and hydrological cycle.

[3] *Kawamura and Kaplan* [1987] identified the automobile exhaust as primary source of OxA. It has been hypothesized that the oxalic acid is produced by photochemical oxidations of reactive organic precursors such as aromatic hydrocarbons [*Kawamura et al.*, 1996b], isoprene [*Lim et al.*, 2005] and acetylene/ethene [*Warneck*, 2003] in the atmosphere. Laboratory experiments also demonstrated the production of OxA by aqueous phase photochemical oxidation of pyruvic acid [*Carlton et al.*, 2006] and glyoxal [*Tan et al.*, 2009], which are proposed to form by the oxidation of reactive organic precursors in gas phase [*Kawamura et al.*, 1996b; *Lim et al.*, 2005; *Warneck*, 2003]. Further, it has also been proposed that the photochemical oxidation of succinic and malonic acids produce OxA in the atmosphere [*Kawamura and Ikushima*, 1993].

[4] Due to the low volatility, oxalic acid is predominantly associated with aerosol particles in the atmosphere, which are scavenged by precipitation typically within 6–12 days [*Balkanski et al.*, 1993]. On the other hand, it can also be removed from the atmosphere by oxidation with OH and NO_3 radical attack in aqueous phase (atmospheric waters). Further, it tends to form a complex with iron in aqueous phase and then undergo decarboxylation reaction yielding CO_2 in the presence of sunlight [*Zuo and Hoigne*, 1994]. Nonetheless, its life cycle and photochemical transformations in the atmosphere remain highly uncertain.

[5] Stable carbon isotopic ratio ($\delta^{13}C$) of specific organic compound is useful to better understand its photochemical processing in ambient air. *Rudolph et al.* [2003] found a substantial enrichment of ^{13}C of isoprene, a precursor of oxalic acid, in locations remote from isoprene emitting vegetation compared to that in locations directly influenced by isoprene emissions. *Wang and Kawamura* [2006] found an increase in $\delta^{13}C$ of OxA and a decrease in its concentration in remote marine aerosols from midlatitudes toward the equator over the western Pacific Ocean and Southern Ocean. Moreover, average $\delta^{13}C$ of OxA precursors such as glyoxylic, malonic, and succinic acids were reported to be lower than that of OxA in atmospheric aerosols [*Aggarwal and Kawamura*, 2008; *Pavuluri et al.*, 2011; *Wang and Kawamura*, 2006]. Thus, $\delta^{13}C$ of OxA seems to be controlled by its photochemical degradation and/or photochemical production from the photochemically aged precursor gases and intermediate compounds.

[6] In this study, we conducted a laboratory experiment with H_2O_2-Fe-UV system in aqueous phase to better understand the changes in $\delta^{13}C$ of OxA with photochemical aging in different type of environments. Here, we provide a laboratory evidence for the isotopic fractionation of ^{13}C in OxA that occurs during photochemical processes.

2. Materials and Methods

2.1. Irradiation Experiment of Oxalic Acid

[7] Batch experiments were conducted for photolysis of authentic oxalic acid (OxA) ($(COOH)_2 \cdot 2H_2O$; Wako,

[1]Institute of Low Temperature Science, Hokkaido University, Sapporo, Japan.

0094-8276/12/2011GL050398

Table 1. Experimental Conditions of UV Irradiation for the Photolysis of Oxalic Acid in Aqueous Phase[a]

	Experiment I OxA+H_2O_2+UV	Experiment II OxA+Fe^{3+}+H_2O_2+UV			Experiment III OxA+Fe^{2+}+H_2O_2+UV
		a	b	c	
Initial Concentration of OxA (μM)	1000	200	1000	4000	1000
Initial Molar Concentration Ratios of OxA and Reagents	1:10	10:1:50	50:1:50	200:1:50	50:1:50
Duration of Experiment (min)	180	90	90	180	90
Control w/o UV	Yes	Yes	No	No	No

[a]OxA = Oxalic acid. Initial pH of experimental solution = 3.5 $\sim$ 3.7. Typical cloud/fog pH = 2–5.

Japan) in aqueous phase in 100 cc quartz reaction vessel (cylinder) for 90 to 180 min. Hydrogen peroxide (H_2O_2, Wako, Japan) was used to produce hydroxyl radical continuously using low pressure mercury lamp (Ushio, UL0-6DQ) that emits a UV with wavelength primarily at 254 nm in all experiments. Iron-III (Fe^{3+}) (Ferric sulfate, $Fe_2(SO_4)_3$; Wako, Japan) and iron-II (Fe^{2+}) (Ferrous sulfate, $FeSO_4 \cdot 7H_2O$; Wako, Japan) species were used to catalyze the photolysis of OxA in Experiments IIa-c and III, respectively (see Table 1 for the experimental system). Initial concentration of OxA ranged from 200 μM to 4000 μM depending on the experimental system (see Table 1). The molar concentration ratio of OxA and H_2O_2 in experimental solution (50 ml) in Experiment I was 1:10. In Experiment IIa-c, the initial concentration ratios of OxA, Fe^{3+} and H_2O_2 were 10:1:50, 50:1:50 and 200:1:50, respectively. In Experiment III, the initial concentration ratio of OxA, Fe^{2+} and H_2O_2 was 50:1:50. All the experiments were conducted at room temperature (26°C) and the temperature variation in experimental chamber was found to be $\leq \pm 2$°C during the experiment. An aliquot (0.5 ml) of sample was taken at different times in each experiment. 15–50 μl of catalase aqueous solution (Worthington, USA) were added to each sample immediately after the experiment to destroy the remaining H_2O_2. Batch samples were diluted to about 20 ml each with Milli Q water and then the available oxalic acid was derivatized to dibutyl oxalate on the same day to measure its concentration and $\delta^{13}C$, as described in the following section.

[8] Two sets of control experiments that correspond to Experiments I and IIa were also conducted by wrapping the reaction vessel with aluminum foil in order to avoid any UV light exposure (Table 1). Furthermore the experimental solution prepared with (i) H_2O_2, (ii) Fe^{3+} + H_2O_2, (iii) Fe^{2+} + H_2O_2 and (iv) authentic OxA were sampled from reaction vessel and analyzed like samples to check a possible contamination from the experimental protocol or the chemicals including catalase. In addition, one more authentic OxA sample was collected from reaction vessel and analyzed without adding catalase for recovery and for its actual $\delta^{13}C$ value measurement.

2.2. Measurement of Oxalic Acid Concentration and Its Stable Carbon Isotopic Ratio

[9] Concentration of oxalic acid (OxA) was determined using a method reported elsewhere [*Kawamura and Ikushima*, 1993]. Briefly, the sample was concentrated to near dryness using a rotary evaporator under vacuum and then derivatized to dibutyl oxalate with 14% BF_3/n-butanol at 100°C. The dibutyl oxalate was extracted with *n*-hexane and then analyzed using a capillary GC-FID (HP 6890). The recovery of authentic oxalic acid was 79% and the analytical error in duplicate analysis was within 9%. The concentrations reported here are not corrected for the recovery.

[10] Stable carbon isotopic ratio ($\delta^{13}C$) of OxA was measured using a method reported by *Kawamura and Watanabe* [2004]. Briefly, an appropriate amount of internal standard (n-C_{13} alkane) was spiked to the part of derivatized fraction of the sample following the amount of oxalic acid dibutyl ester and then injected to GC (HP6890)/isotope ratio mass spectrometry (GC/irMS) (Finnigan MAT Delta Plus) for the measurement of $\delta^{13}C$ value of the dibutyl oxalate. The $\delta^{13}C$ value of oxalic acid in the sample was then calculated using an isotopic mass balance equation based on the measured $\delta^{13}C$ value of the oxalate and derivatizing agent (1-butanol) [*Kawamura and Watanabe*, 2004]. Difference in $\delta^{13}C$ of free acid for duplicate analysis was generally below 1‰.

2.3. Validation of the Method

[11] Procedural blanks for OxA in (i) H_2O_2, (ii) Fe^{3+} + H_2O_2 and (iii) Fe^{2+} + H_2O_2 were checked and the amounts of OxA were found to be negligible (0–0.37 μM). The addition of catalase to authentic OxA sample also did not cause any contamination of OxA, and the recovery (81%) of OxA in the presence of catalase was comparable to that (79%) of authentic OxA. These results indicate that the methodology adopted for this experiment is satisfactory. Stable carbon isotopic ratio ($\delta^{13}C$) of authentic OxA was found to be -21.65‰, which is comparable to that (-22.25 ± 0.48‰) reported previously for the authentic OxA obtained from the same source (Wako, Japan) [*Kawamura and Watanabe*, 2004]. The $\delta^{13}C$ value of OxA in experimental sample collected right at the beginning of experiments was found to be -24.65‰ in Experiment I, -24.90‰ in Experiment II and -16.90‰ in Experiment III. Unfortunately, the mechanisms involved in depletion of ^{13}C in Experiment I and II and enrichment of ^{13}C in Experiment III cannot be explained at this moment. However, a trend of ^{13}C enrichment was found in the remaining OxA for each experiment as discussed below. Thus, we consider that the trends of $\delta^{13}C$ of OxA with photochemical aging are meaningful.

2.4. Calculation of the Kinetic Isotope Effect

[12] The kinetic isotope effect (KIE), defined as the ratio of the rate constants for the species containing only ^{12}C atoms and those containing a ^{13}C atom (k_{12}/k_{13}), was calculated following the technique described by *Anderson et al.* [2003]. The k_{12}/k_{13} ratio can be obtained from the slope of the linear least-square fit of the relationship between concentration and stable carbon isotopic ratios ($\delta^{13}C$) of the studied compound. This relationship can be described by the following equation:

$$\ln(C_t/C_0) = k_{12}/k_{13}/(1 - k_{12}/k_{13}) \ln\left[\left({}^{13}C_t/{}^{12}C_t\right)/\left({}^{13}C_0/{}^{12}C_0\right)\right] \quad (1)$$

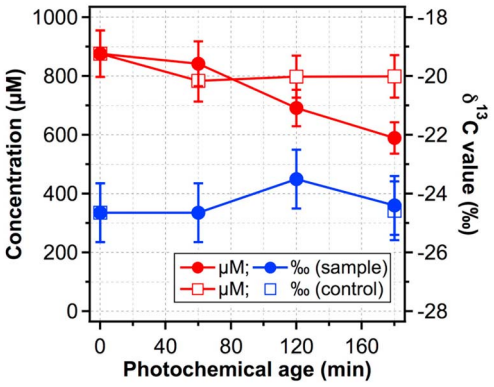

Figure 1. Changes in the concentration and stable carbon isotopic ratio ($\delta^{13}C$) of oxalic acid (OxA) with photochemical aging (irradiation time) under H_2O_2-UV system in aqueous phase at molar concentration ratios of OxA:H_2O_2 = 1:10. Bars represent the analytical error in concentration and difference in $\delta^{13}C$ measurements in duplicate analysis.

where C_t and C_0 correspond to the concentration and $^{13}C_t/^{12}C_t$ and $^{13}C_0/^{12}C_0$ correspond to the $\delta^{13}C$ of the studied compound (OxA) at time t and zero, respectively. The experimental uncertainty for an individual experiment can be determined from the uncertainty in the slope.

[13] Isotopic fractionation effects are often very small and therefore they can be expressed as a relative difference of the reaction rate constants in epsilon (ε) notation as per mil values, similar to using $\delta^{13}C$ values to express stable carbon isotopic ratios, for the sake of convenience [*Anderson et al.*, 2003]:

$$\varepsilon(‰) = (k_{12} - k_{13})/k_{12} \times 1000 = (k_{12}/k_{13} - 1) \times 1000 \quad (2)$$

3. Results and Discussion

3.1. Decomposition of Oxalic Acid in H_2O_2-UV System

[14] Figure 1 shows changes in the concentration and $\delta^{13}C$ of oxalic acid (OxA) as a function of photochemical aging (that is, irradiation time) in the H_2O_2-UV system (Experiment I). The concentration of OxA gradually decreased to 67% of the initial concentration in 180 min period of irradiation (Figure 1), but it was not significant in the control experiment without irradiation (see Figure 1), indicating that the photochemical degradation of OxA by OH radical attack and/or UV photolysis is significant (see Table 2). This experimental evidence may imply a photochemical oxidation of OxA to CO_2 by OH radical in the atmosphere, as has been proposed in model studies [*Lim et al.*, 2005; *Warneck*, 2003).

[15] Surprisingly, the results did not show any significant change in $\delta^{13}C$ of OxA with photochemical aging under the conditions of OH radical attack (Figure 1). Further, as can be seen from Figure 2, the linear dependence between concentration and $\delta^{13}C$ of OxA according to equation (1) was found to be negligible, indicating that the isotopic fractionation is insignificant. However, we do not preclude the significant isotopic fractionation on prolonged aging, because unidirectional chemical reactions generally show an enrichment of ^{12}C in reaction products with the remaining reactants being isotopically heavier [*Hoefs*, 1997; *Rudolph et al.*, 2000] and the observed decomposition rates; 10 nM s^{-1}, 26 nM s^{-1} and 27 nM s^{-1} at 60 min, 120 min and 180 min, respectively, indicate that the photochemical degradation under OH radical attack may become more effective at lower levels of OxA that may lead to significant enrichment of ^{13}C in the remaining OxA.

Table 2. Kinetic Isotope Effects (KIE) for the Photolysis of Oxalic Acid in Different Experiments under H_2O_2-Fe^{3+}(Fe^{2+})-UV System in Aqueous Phase[a]

Experiment	KIE ± SD (‰)	R^2	k (L $mole^{-1}$ s^{-1})
I			0.054
IIa			205.7
IIb	3.20 ± 0.49	0.94	1.149
IIc	21.62 ± 5.41	0.95	0.007
III	2.18 ± 1.18	0.73	0.385

[a]SD = Standard deviation, estimated from the uncertainty of the slope of the linear regression according to equation (1).

3.2. Photolysis of Oxalic Acid in the Presence of Fe^{3+}

[16] Figure 3a–3c shows changes in the concentration and $\delta^{13}C$ of OxA with photochemical aging in the presence of Fe^{3+} (Experiment II). The photochemical degradation of OxA was found to be very fast when the initial molar concentration ratio of OxA and Fe^{3+} was 10:1 (Experiment IIa; Figure 3a), however it became slow with an increase in the initial concentration ratios to 50:1 (Experiment IIb; Figure 3b) and 200:1 (Experiment IIc; Figure 3c), because the initial decomposition rates of OxA in Experiment IIa-c (453 nM s^{-1} and 382 nM s^{-1} at 5 min and 420 nM s^{-1} at 15 min, respectively) were comparable although the over-all rates (30 nM s^{-1} and 129 nM s^{-1} in 90 min and 82 nM s^{-1} in 180 min; Table 2) were different. *Zuo and Hoigne* [1994] also reported that OxA undergo fast photochemical

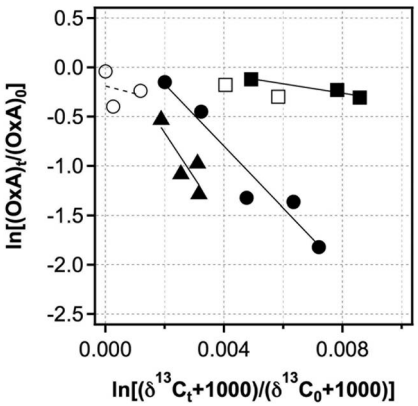

Figure 2. A plot of linear least squares fit of the data from Experiment I (open circles), Experiment IIb (solid circles) and IIc (solid squares), and III (solid triangles) according to equation (1) for the photolysis of oxalic acid (OxA) under H_2O_2-Fe^{3+}(Fe^{2+})-UV system in aqueous phase. $\ln[(\delta^{13}C+1000)/(\delta^{13}C+1000)]$ is equivalent to $\ln[(^{13}C_t/^{12}C_t)/(^{13}C_0/^{12}C_0)]$. Two data points (open squares) in Experiment IIc, which were found to be the outliers, are omitted for linear fit.

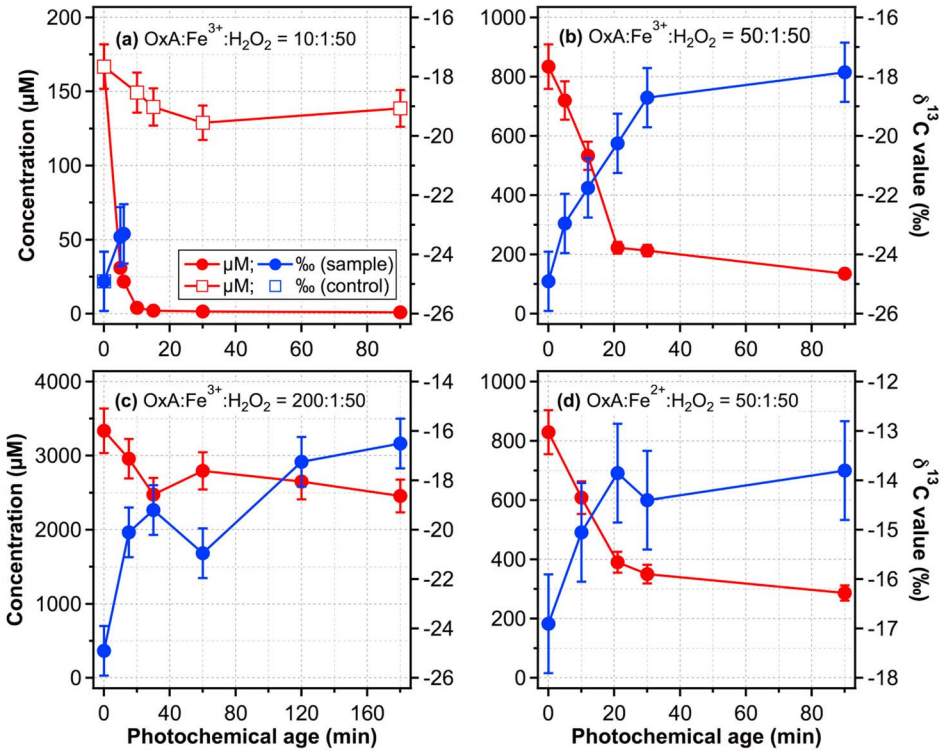

Figure 3. Changes in the concentration and stable carbon isotopic ratio ($\delta^{13}C$) of oxalic acid (OxA) with photochemical aging (irradiation time) under H_2O_2-Fe^{3+}(Fe^{2+})-UV system in aqueous phase at different molar concentration ratios of (a) OxA:Fe^{3+}:H_2O_2 = 10:1:50, (b) OxA:Fe^{3+}:H_2O_2 = 50:1:50 and (c) OxA:Fe^{3+}:H_2O_2 = 200:1:50 and (d) OxA:Fe^{2+}:H_2O_2 = 50:1:50. Bars represent the analytical error in concentration and difference in $\delta^{13}C$ measurements in duplicate analysis.

decomposition (10 ± 1 nM s^{-1}) in the presence of Fe^{3+} in atmospheric waters and the rate depends on the concentration of Fe^{3+} species, reaching to the maximum at 1:1 ratio of OxA and Fe^{3+}.

[17] It is well documented that OxA tends to form a complex with Fe^{3+} by acting as ligand in aqueous phase and then produces Fe^{2+} and oxalate radical ($C_2O_4^-$) by electron transfer to the Fe^{3+} upon the absorption of sunlight [*Zuo and Hoigne*, 1994]. The formed $C_2O_4^-$ radical may undergo a decarboxylation reaction yielding CO_2 and CO_2^- radical, a strong reductant that can reduce a molecular O_2 or an additional Fe^{3+}-oxalato complex. Thus, Fe^{3+} acts as a catalyst for the photolysis of OxA, which significantly depends on light intensity, pH and concentrations [*Zuo and Hoigne*, 1994], and could cause the isotopic fractionation in OxA.

[18] In fact, the OxA decomposition rates obtained in first 5–15 min in H_2O_2-Fe^{3+}-UV system in this study were higher by a factor of ca. 25∼40 than that reported for Fe^{3+}-UV system (10 nM s^{-1}) [*Zuo and Hoigne*, 1994]. It is also of noteworthy that the OxA has degraded to some extent in control experiment (by 17% in 90 min; Figure 3a), in which the concentration of Fe^{3+} was high (OxA: Fe^{3+} = 10:1). These indicate that the photolysis of OxA catalyzed by Fe^{3+} is more effective in OH radical-enriched environment, and is also possible for some extent even in the absence of UV.

[19] $\delta^{13}C$ values of OxA were found to increase with photochemical processing due to photochemical decomposition of OxA catalyzed by Fe^{3+} (Figures 3a–3c). In Experiment IIa, $\delta^{13}C$ has been measured in only first three samples collected right at the beginning and at 5 min and 6 min, because the available amount of OxA was insufficient for the $\delta^{13}C$ measurement in most of the samples. Although 81% of OxA has been degraded in 5 min of irradiation, the enrichment of ^{13}C in the remained OxA was found to be only 1.5‰ in Experiment IIa (Figure 3a). On the other hand, the enrichment of ^{13}C in irradiated OxA samples was very high in Experiments IIb (ca. 7‰ in 90 min) and IIc (ca. 8‰ in 180 min), in which 84% and 26% of OxA have been decomposed, respectively. Further they showed an enhanced enrichment of ^{13}C in the remaining OxA with photochemical aging (Figure 3b and 3c).

[20] A linear dependence between concentration and $\delta^{13}C$ of OxA according to equation (1) has been found in Experiment IIb and c (Figure 2). In fact, the data points of concentration and $\delta^{13}C$ of OxA in sample 3 and 4 in Experiment IIc, respectively, were found to be the outliers and hence those data points were excluded from linear fit (Figure 2) in order to avoid an adverse effect on the overall quality of the fit. The kinetic isotope effect (KIE) of OxA was found to be 3.2 ± 0.49‰ in Experiment IIb and 21.62 ± 5.41‰ in Experiment IIc. Unfortunately, the KIE could not be estimated in Experiment IIa due to insufficient number of observations available for $\delta^{13}C$. Interestingly, the KIE of OxA found in Experiment IIc is comparable to that (18.85 ± 2.80‰) of ethene, a precursor for OxA [*Warneck*, 2003], during its reaction with ozone [*Iannone et al.*, 2003]. Thus, the results from Experiment IIa-c clearly imply that the isotopic fractionation in OxA during its photolysis catalyzed

by Fe^{3+} is enhanced with an increase in the initial concentration ratios of OxA to Fe^{3+} and photochemical aging. Further the role of percent degradation of OxA in the given photochemical age rather insignificant.

3.3. Photolysis of Oxalic Acid Under Fe^{2+}-H_2O_2-UV System

[21] Changes in the concentration of OxA and its $\delta^{13}C$ as a function of photochemical aging in the presence of Fe^{2+} (Experiment III) are shown in Figure 3d. The OxA concentrations decreased with aging (Figure 3d), indicating that photolysis of OxA catalyzed by Fe^{2+} is also significant. This trend is similar to that obtained in Experiment IIa (catalyzed by Fe^{3+}; Figure 3a), in which the concentration ratios of OxA and iron species were same as in Experiment III (50:1). However, the degradation rates of OxA were found to be always lower in Experiment III (65% in 90 min) than in Experiment IIa (84% in 90 min) (Table 2) at a given photochemical age (irradiation time). In fact, the Fe^{2+}-oxalato complex undergoes a charge transfer from the Fe^{2+} to the surrounding solvent molecule upon the absorption of UV light, forming Fe^{3+}-oxalato complex [*Zuo and Deng*, 1997]. Thus, the initial photochemical reaction of Fe^{2+}-oxalato complexes does not directly lead to the decomposition, but leads to an induction period in photooxidation of OxA catalyzed by Fe^{2+} [*Zuo and Deng*, 1997].

[22] $\delta^{13}C$ values of the remaining OxA also increased with photochemical aging in Experiment III (Figure 3d) and showed a linear dependence between concentration and $\delta^{13}C$ according to equation (1) (Figure 2). However, the enrichment of ^{13}C (ca. 3‰) in 90 min period of irradiation in Experiment III was lower than that (ca. 7‰) in Experiment IIb, in which the concentration ratios of OxA to iron were the same (50:1). In fact, the KIE in experiment III (2.18 ± 1.18‰) was comparable to that in Experiment IIb (3.2 ± 0.49‰). However, the high uncertainty associated with KIE in Experiment III compared to that in Experiment IIb suggests that the isotopic fractionation was relatively lower in the former than that in the latter. Although the reason behind this difference in ^{13}C enrichment of OxA is not clear, we presume that ^{12}C may be more efficiently involved in subsequent photochemical reactions of Fe^{3+}-oxalato complexes than in those of Fe^{2+}-oxalato complexes because Fe^{3+}-oxalato complexes absorb the UV light more efficiently than Fe^{2+}-oxalato complexes do [*Zuo and Deng*, 1997].

4. Conclusions

[23] Based on the results obtained from the batch experiments on laboratory photolysis of OxA under H_2O_2-UV system in aqueous phase, we found that the OH radical attack decomposes the OxA significantly but has no significant effect on its stable carbon isotopic composition ($\delta^{13}C$). However, the isotopic fractionation may become significant on prolonged aging and/or at low levels of OxA. In contrast, under H_2O_2-Fe-UV system, photochemical decomposition of OxA in the presence of Fe^{3+} showed a significant enrichment of ^{13}C in the remaining OxA that strongly depends on concentration ratios of OxA and Fe^{3+} in a given environment and photochemical aging. Fe^{2+} species also catalyze the photolysis of OxA being similar to that of Fe^{3+} although the enrichment of ^{13}C is smaller. These results support an increase in $\delta^{13}C$ values of OxA that has been observed in the remote marine aerosols [*Wang and Kawamura*, 2006], and useful to assess the photochemical processes of aerosols through atmospheric isotopic measurements.

[24] **Acknowledgments.** This study was partly supported by a grant-in-aid 19204055 from the Japan Society for the Promotion of Science (JSPS) and the Environment Research and Technology Development Fund (B-0903) of the Ministry of the Environment, Japan. We appreciate the financial support of a JSPS Fellowship to C. M. P. We also thank E. Tachibana for isotopic measurement of OxA.

[25] The Editor thanks Jochen Rudolph and an anonymous reviewer for their assistance in evaluating this paper.

References

Aggarwal, S. G., and K. Kawamura (2008), Molecular distributions and stable carbon isotopic compositions of dicarboxylic acids and related compounds in aerosols from Sapporo, Japan: Implications for photochemical aging during long-range atmospheric transport, *J. Geophys. Res.*, *113*, D14301, doi:10.1029/2007JD009365.

Anderson, R. S., E. Czuba, D. Ernst, L. Huang, A. E. Thompson, and J. Rudolph (2003), Method for measuring carbon kinetic isotope effects of gas-phase reactions of light hydrocarbons with the hydroxyl radical, *J. Phys. Chem. A*, *107*, 6191–6199, doi:10.1021/jp034256d.

Balkanski, Y. J., D. J. Jacob, G. M. Gardner, W. C. Graustein, and K. K. Turekian (1993), Transport and residence times of tropospheric aerosols inferred from a global three-dimensional simulation of ^{210}Pb, *J. Geophys. Res.*, *98*(D11), 20,573–20,586, doi:10.1029/93JD02456.

Carlton, A. G., B. J. Turpin, H.-J. Lim, and K. E. Alteri (2006), Link between isoprene and secondary organic aerosol (SOA): Pyruvic acid oxidation yields low volatility organic acids in clouds, *Geophys. Res. Lett.*, *33*, L06822, doi:10.1029/2005GL025374.

Ho, K. F., J. J. Cao, S. C. Lee, K. Kawamura, R. J. Zhang, J. C. Chow, and J. G. Watson (2007), Dicarboxylic acids, ketocarboxylic acids, and dicarbonyls in the urban atmosphere of China, *J. Geophys. Res.*, *112*, D22S27, doi:10.1029/2006JD008011.

Hoefs, J. (1997), *Stable Isotope Geochemistry*, Springer, New York.

Iannone, R., R. S. Anderson, J. Rudolph, L. Huang, and D. Ernst (2003), The carbon kinetic isotope effects of ozone-alkene reactions in the gas-phase and the impact of ozone reactions on the stable carbon isotope ratios of alkenes in the atmosphere, *Geophys. Res. Lett.*, *30*(13), 1684, doi:10.1029/2003GL017221.

Kawamura, K., and K. Ikushima (1993), Seasonal changes in the distribution of dicarboxylic acids in the urban atmosphere, *Environ. Sci. Technol.*, *27*, 2227–2235, doi:10.1021/es00047a033.

Kawamura, K., and I. R. Kaplan (1987), Motor exhaust emissions as a primary source for dicarboxylic acids in Los Angeles ambient air, *Environ. Sci. Technol.*, *21*, 105–110, doi:10.1021/es00155a014.

Kawamura, K., and K. Usukura (1993), Distributions of low molecular weight dicarboxylic acids in the North Pacific aerosol samples, *J. Oceanogr.*, *49*, 271–283, doi:10.1007/BF02269565.

Kawamura, K., and T. Watanabe (2004), Determination of stable carbon isotopic compositions of low molecular weight dicarboxylic acids and ketocarboxylic acids in atmospheric aerosol and snow samples, *Anal. Chem.*, *76*, 5762–5768, doi:10.1021/ac049491m.

Kawamura, K., T. Seméré, Y. Imai, Y. Fujii, and M. Hayashi (1996a), Water soluble dicarboxylic acids and related compounds in Antarctic aerosols, *J. Geophys. Res.*, *101*(D13), 18,721–18,728, doi:10.1029/96JD01541.

Kawamura, K., H. Kasukabe, and L. A. Barrie (1996b), Source and reaction pathways of dicarboxylic acids and dicarbonyls in Arctic aerosols: one year of observations, *Atmos. Environ.*, *30*, 1709–1722, doi:10.1016/1352-2310(95)00395-9.

Kundu, S., K. Kawamura, T. W. Andreae, A. Hoffer, and M. O. Andreae (2010), Molecular distributions of dicarboxylic acids, ketocarboxylic acids and α-dicarbonyls in biomass burning aerosols: Implications for photochemical production and degradation in smoke layers, *Atmos. Chem. Phys.*, *10*, 2209–2225, doi:10.5194/acp-10-2209-2010.

Lim, H.-J., A. G. Carlton, and B. J. Turpin (2005), Isoprene forms secondary organic aerosol through cloud processing: Model simulations, *Environ. Sci. Technol.*, *39*, 4441–4446, doi:10.1021/es048039h.

Pavuluri, C. M., K. Kawamura, T. Swaminathan, and E. Tachibana (2011), Stable carbon isotopic compositions of total carbon, dicarboxylic acids and glyoxylic acid in the tropical Indian aerosols: Implications for sources and photochemical processing of organic aerosols, *J. Geophys. Res.*, *116*, D18307, doi:10.1029/2011JD015617.

Peng, C., M. N. Chan, and C. K. Chan (2001), The hygroscopic properties of dicarboxylic and multifunctional acids: Measurements and UNIFAC

predictions, *Environ. Sci. Technol.*, *35*, 4495–4501, doi:10.1021/es0107531.

Rudolph, J., E. Czuba, and L. Huang (2000), The stable carbon isotope fractionation for reactions of selected hydrocarbons with OH-radicals and its relevance for atmospheric chemistry, *J. Geophys. Res.*, *105*(D24), 29,329–29,346, doi:10.1029/2000JD900447.

Rudolph, J., R. S. Anderson, K. V. Czapiewski, E. Czuba, D. Ernst, T. Gillespie, L. Huang, C. Rigby, and A. E. Thompson (2003), The stable carbon isotope ratio of biogenic emissions of isoprene and the potential use of stable isotope ratio measurements to study photochemical processing of isoprene in the atmosphere, *J. Atmos. Chem.*, *44*, 39–55, doi:10.1023/A:1022116304550.

Saxena, P., L. M. Hildemann, P. H. McMurry, and J. H. Seinfeld (1995), Organics alter hygroscopic behavior of atmospheric particles, *J. Geophys. Res.*, *100*(D9), 18,755–18,770, doi:10.1029/95JD01835.

Tan, Y., M. J. Perri, S. P. Seitzinger, and B. J. Turpin (2009), Effect of precursor concentration and acidic sulfate in aqueous glyoxal-OH radical oxidation and implications for secondary organic aerosols, *Environ. Sci. Technol.*, *43*, 8105–8112, doi:10.1021/es901742f.

Wang, H., and K. Kawamura (2006), Stable carbon isotopic composition of low-molecular-weight dicarboxylic acids and ketoacids in remote marine aerosols, *J. Geophys. Res.*, *111*, D07304, doi:10.1029/2005JD006466.

Warneck, P. (2003), In-cloud chemistry opens pathway to the formation of oxalic acid in the marine atmosphere, *Atmos. Environ.*, *37*, 2423–2427, doi:10.1016/S1352-2310(03)00136-5.

Zuo, Y., and Y. Deng (1997), Iron(II)-catalyzed photochemical decomposition of oxalic acid and generation of H_2O_2 in atmospheric liquid phases, *Chemosphere*, *35*(9), 2051–2058, doi:10.1016/S0045-6535(97)00228-2.

Zuo, Y., and J. Hoigne (1994), Photochemical decomposition of oxalic, glyoxalic and pyruvic acid catalysed by iron in atmospheric waters, *Atmos. Environ.*, *28*(7), 1231–1239, doi:10.1016/1352-2310(94)90270-4.

K. Kawamura and C. M. Pavuluri, Institute of Low Temperature Science, Hokkaido University, N19, W08, Kita-ku, Sapporo, Hokkaido 060-0819, Japan. (kawamura@lowtem.hokudai.ac.jp)